3D Optimal Design of Transformer Tank Shields using Design Sensitivity Analysis

Yingying Yao*, Jae Seop Ryu, Chang Seop Koh**, and Dexin Xie****

Abstract - A novel 3D shape optimization algorithm is presented for electromagnetic devices carrying eddy current. The algorithm integrates the 3D finite element performance analysis and the steepest descent method with design sensitivity and mesh relocation method. For the design sensitivity formula, the adjoint variable vector is defined in complex form based on the 3D finite element method for eddy current problems. A new 3D mesh relocation method is also proposed using the deformation theory of the elastic body under stress to renew the mesh as the shape changes. The design sensitivity for the surface nodal points is also systematically converted into that for the design variables for the parameterized optimization application. The proposed algorithm is applied to the optimum design of the tank shield model of the transformer and the effectiveness is proved.

Keywords: shape optimization, mesh regeneration, design sensitivity, deformation theory, eddy current, transformer

1. Introduction

During the last decade, both the deterministic and non-deterministic methods of optimization algorithms have been developed and successfully applied to engineering design problems. The non-deterministic optimization method, such as the genetic algorithm and the evolution strategy, has been applied extensively because it often provides a global optimum solution and can be easily combined with an existing finite element performance analysis program. On the other hand, through the deterministic methods, such as the gradient method incorporated with design sensitivity analysis, sometimes falls into a local minima, it has been preferred since it requires fewer computations of the objective function value [1, 2]. For the 3D shape optimal design, the deterministic method combined with design sensitivity analysis is therefore thought to be a good choice.

Design sensitivity analysis, which gives the gradient vector of the objective function with respect to the design variable, is well developed and successfully applied to various 2D shape optimization problems [3-10]. For 3D problems, however, the application is limited to the magnetostatic problem [1, 7]. The 3D design sensitivity formula was first derived for magnetostatic problems using the boundary element method and applied to the design of simple electromagnet [7]. With the finite element method, the 3D design sensitivity formula is also derived in [1], where the adjoint variable is evaluated using the existing performance analysis code for every design variable. Thus the calculation of the design sensitivity is computationally very expensive.

Another important part of the shape optimal design is renewing the finite element mesh as the design variables change. In this process, the mesh distortion must be minimized to get an accurate finite element analysis result, and the newly generated mesh should maintain the same topology with the previous mesh [11]. There are two kinds of finite element mesh renewing methods. One is to regenerate a new mesh according to the changed design variables using an automatic mesh generator. This method may guarantee the quality of the finite element mesh, but the integration with the performance analysis code and getting a topologically exact mesh is difficult. The other is to modify the latest mesh so that the mesh distortion is minimized and the same topology is maintained. In the early research for 2D shape optimization, the finite element mesh modification method using the deformation theory of the elastic body is well derived [11].

In this paper, a design sensitivity formula for the 3D eddy current problem is derived in complex form using the finite element and adjoint variable methods. In the finite element analysis, the A, $A-\phi$ method is employed and one calculation of the adjoint variable is enough for the design sensitivity formula. Therefore, as the number of design variable increases, few extra computations are required. A 3D mesh regeneration method, based on the deformation of the elastic body under stress, is also presented. Using the method, a topologically constant 3D mesh with

* School of Electrical Engineering, Shenyang University of Technology, Shenyang, P.R.China.(yaoying62@hotmail.com)
** School of Electrical and Computer Engineering, Chungbuk National University, Cheongju, Chungbuk, Korea. (kohcs@chungbuk.ac.kr)
Received July 29, 2002; Accepted January 16, 2003

relatively good quality is obtained. Finally, a 3D shape optimal design algorithm is developed by integrating the finite element performance analysis, the steepest descent method with design sensitivity, and the mesh relocation method. The developed algorithm is applied to the optimal design of the transformer tank shield model.

2. Design Sensitivity for the 3D Eddy Current Problem

The governing equations for the 3D electromagnetic system with time harmonic excitation of frequency ω are given as follows [12]:

$$\begin{aligned}&\nabla\times\left(\nu\nabla\times\dot{\mathbf{A}}\right)-\nabla\left(\nu\nabla\cdot\dot{\mathbf{A}}\right)+j\omega\sigma\dot{\mathbf{A}}+\sigma\nabla\dot{\phi}=0\\&\nabla\cdot\left(-j\omega\sigma\dot{\mathbf{A}}-\sigma\nabla\dot{\phi}\right)=0\end{aligned}\quad \text{in } V_1 \qquad (1)$$

$$\nabla\times\left(\nu\nabla\times\dot{\mathbf{A}}\right)-\nabla\left(\nu\nabla\cdot\dot{\mathbf{A}}\right)=\dot{\mathbf{J}}_s \qquad \text{in } V_2 \qquad (2)$$

where V_1 and V_2 are regions that contain the eddy current and exciting current, respectively. Through the finite element formulation, the governing equations result in the following complex matrix equation:

$$[\dot{S}][\dot{X}]=[\dot{Q}]. \qquad (3)$$

The shape optimization problem for the system including eddy current can be generally expressed as

$$\begin{aligned}&\textit{Minimize } F(p)=F(p,\dot{X},\dot{X}^*),\\&\textit{Subject to } [p]^L\le[p]\le[p]^U\end{aligned} \qquad (4)$$

where F is the objective function, $[p]$ is the design variable vector composed of the surface nodal points, $\dot{X}$ and $\dot{X}^*$ are the real and imaginary parts of the state variable, respectively, and $[p]^L$ and $[p]^U$ are the lower and upper limitations of the design variable, respectively. The design sensitivity of the objective function with respect to the design variables can be written, using complex analysis, as

$$\begin{aligned}\frac{dF}{d[p]^T}&=\frac{\partial F}{\partial[p]^T}+\frac{\partial F}{\partial[\dot{X}]^T}\frac{\partial[\dot{X}]}{\partial[p]^T}+\frac{\partial F}{\partial[\dot{X}]^{*T}}\frac{\partial[\dot{X}]^*}{\partial[p]^T}\\&=\frac{\partial F}{\partial[p]^T}+\frac{\partial F}{\partial[X_R]^T}\frac{\partial[X_R]}{\partial[p]^T}+\frac{\partial F}{\partial[X_I]^T}\frac{\partial[X_I]}{\partial[p]^T}\\&=\frac{\partial F}{\partial[p]^T}+2\mathrm{Re}\left(\frac{\partial F}{\partial[\dot{X}]^T}\frac{d[\dot{X}]}{d[p]^T}\right)\end{aligned} \qquad (5)$$

where the subscripts R and I denote the real and imaginary part, respectively, and the superscript * means the conjugate. After differentiating both sides of (3) with respect to $[p]$ and multiplying an adjoint variable vector $[\lambda]^T$, we get

$$[\lambda]^T[\dot{S}]\frac{d[\dot{X}]}{d[p]}=[\lambda]^T\frac{d}{d[p]}\left(\dot{Q}-[S][\dot{X}]\right). \qquad (6)$$

The adjoint variable may be chosen so that the coefficients of $d[\dot{X}]/d[p]$ in (5) and (6) are equal, and it may be defined as

$$[\dot{S}]^T[\lambda]=\frac{\partial F}{\partial\dot{X}} \qquad (7)$$

where it can be seen that the adjoint variable $[\lambda]$ is independent of the number of design variables. The design sensitivity formula are finally derived as

$$\frac{dF}{d[p]^T}=\frac{\partial F}{\partial[p]^T}+2\mathrm{Re}\left([\lambda]^T\frac{\partial}{\partial[p]^T}\left[[\dot{Q}]-[S][\tilde{\dot{X}}]\right]\right) \qquad (8)$$

where $[\tilde{\dot{X}}]$ is the solution of (3).

The design variables are renewed, using the computed design sensitivity, as

$$[p]_{new}=[p]_{old}-\alpha F(p)\frac{dF}{d[p]^T}\Big/\left|\frac{dF}{d[p]^T}\right|^2 \qquad (9)$$

where α is the relaxation factor.

3. Parameterization of the Tank Shield

In the design sensitivity formula, the design variables are assumed to be surface nodal points. When the shape is parameterized, the design variables are not the surface nodal points themselves but the parameters. The design sensitivity for the design variables, hence, should be computed by using those for the surface nodal points. In this paper, the tank shield of the transformer is parameterized in the following two ways. The first parameterization is achieved, as shown in Fig. 1, using the linear functions. In this case, the coordinate of the nodal point on the design surface is given as

$$x_i=L-x_k+\frac{L_{k+1}-L_k}{y^0_{k+1}-y^0_k}(y_i-y^0_k)\quad\text{when}\quad y^0_{k-1}\le y_i\le y^0_k \qquad (10)$$

where (x_i,y_i) are the coordinates of node i and L,L_k,y^0_k

are explained in Fig.1. The design variables are defined as the vertices $L_k (k = 1,2,3,4)$.

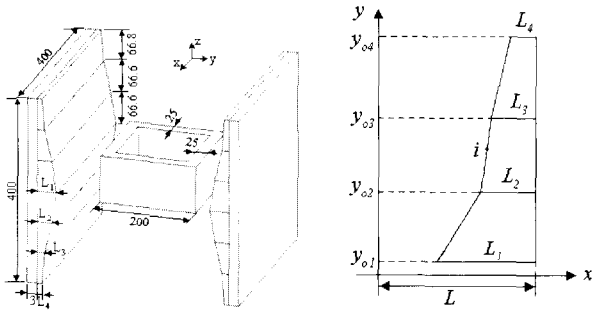

(a) (b)

Fig. 1 Parameterization of the tank shield using linear functions: (a) overall view, (b) parameters.

Another parameterization is done, as shown in Fig. 2, using the step functions. In this case, the coordinates of the nodal point on the design surface are expressed as

$$x_i = L - L_k \quad \text{when} \quad y_{k-1}^0 \le y_i \le y_k^0 \tag{11}$$

where (x_i, y_i) are the coordinates of node i and L, L_k, y_k^0 are shown in Fig. 2. The thickness of each step, $L_k (k = 1,2,3,4)$, is taken as a design variable.

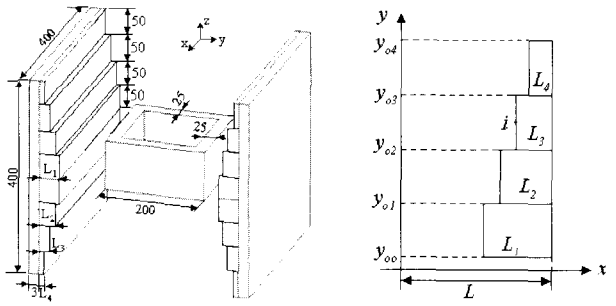

(a) (b)

Fig. 2 Parameterization of the tank shield using step functions. (a) overall view, (b) parameters

The relationship between the design variables and the coordinates of the nodal points on the design surface can be written in the following matrix form from (10) and (11):

$$[p] = [p_0] + [\phi][C] \tag{12}$$

where $[p]$ is the vector composed of the coordinates of the nodal points on the design surface, the coefficient matrix $[\phi]$ is $(ns \times 4)$ if the number of the nodal points on the design surface is ns, and $[C]$ is the design variable vector.

The design sensitivity for the design variable can be computed using (8) and (12) as follows:

$$\frac{dF}{d[C]} = \frac{dF}{d[p]} \frac{\partial [p]}{\partial [C]} = \frac{dF}{d[p]} [\phi]. \tag{13}$$

4. Mesh Regeneration using Structural Deforming Analysis

The strain vector of an elastic body in 3D structural analysis is defined as [13]

$$\varepsilon = \left[\frac{\partial u_x}{\partial x}, \frac{\partial u_y}{\partial y}, \frac{\partial u_z}{\partial z}, \frac{\partial u_x}{\partial y} + \frac{\partial u_y}{\partial x}, \frac{\partial u_y}{\partial z} + \frac{\partial u_z}{\partial y}, \frac{\partial u_z}{\partial x} + \frac{\partial u_x}{\partial z} \right]^T \tag{14}$$

where, if the tetrahedral elements are employed, the displacement vector is defined as

$$\begin{aligned} \mathbf{u} &= u_x(x,y,z)\vec{x} + u_y(x,y,z)\vec{y} + u_z(x,y,z)\vec{z} \\ &= \sum_{i=1}^{4} \mathbf{N}_i \mathbf{a}_i^e = \left[\mathbf{I}N_i, \mathbf{I}N_j, \mathbf{I}N_m, \mathbf{I}N_p \right] \mathbf{a}^e \end{aligned} \tag{15}$$

where $\mathbf{I}$ is the (3x3) identity matrix; $\mathbf{a}^e = \left[\mathbf{a}_i^e, \mathbf{a}_j^e, \mathbf{a}_m^e, \mathbf{a}_p^e \right]^T$; i, j, m and p are the nodal points consisting of an element, $\mathbf{a}_i^e = \left[u_{ix}, u_{iy}, u_{iz} \right]^T$; and the shape function N_i is defined as

$$N_i = (a_i + b_i x + c_i y + d_i z)/6V \tag{16}$$

where V is the volume of the element and the other symbols are defined as follows:

$$\begin{aligned} a_i = (-1)^i \{ & x_j(y_p z_m - y_m z_p) + x_m(y_j z_p - y_p z_j) \\ & + x_p(y_m z_j - y_j z_m) \} \end{aligned} \tag{17-a}$$

$$b_i = (-1)^i \{ y_j(z_m - z_p) + y_m(z_p - z_j) + y_p(z_j - z_m) \} \tag{17-b}$$

$$c_i = (-1)^i \{ z_j(x_m - x_p) + z_m(x_p - x_j) + z_p(x_j - x_m) \} \tag{17-c}$$

$$d_i = (-1)^i \{ x_j(y_m - y_p) + x_m(y_p - y_j) + x_p(y_j - y_m) \}. \tag{17-d}$$

The relationship between the strain and stress for the linear elastic material is given as [13]

$$\sigma = \mathbf{D}(\varepsilon - \varepsilon_0) + \sigma_0 \tag{18}$$

where σ_0 and ε_0 are the initial residual stress and initial strain, respectively; the stress σ consists of direct and shear; and $\mathbf{D}$ is the elasticity matrix given as

$$D=\frac{E(1-\nu)}{(1+\nu)(1-2\nu)}\begin{bmatrix} 1 & \frac{\nu}{(1-\nu)} & \frac{\nu}{(1-\nu)} & 0 & 0 & 0 \\ & 1 & \frac{\nu}{(1-\nu)} & 0 & 0 & 0 \\ & & 1 & 0 & 0 & 0 \\ & & & \frac{(1-2\nu)}{2(1-\nu)} & 0 & 0 \\ & & & & \frac{(1-2\nu)}{2(1-\nu)} & 0 \\ & & \text{symmetric} & & & \frac{(1-2\nu)}{2(1-\nu)} \end{bmatrix} \quad (19)$$

where E is modulus and ν is Poisson's ratio.

Applying the finite element method with tetrahedral elements to (14) and (18), the matrix equation is obtained as

$$[\mathbf{K}]\{\mathbf{a}\}=[\mathbf{f}] \quad (20)$$

where $\{\mathbf{a}\}=\{\mathbf{a_1},\cdots,\mathbf{a_N}\}^T$ is the displacement of each node, $[\mathbf{f}]$ is the forcing load vector, and $[\mathbf{K}]$ is the stiffness matrix determined by the geometry and material constants of the elastic body as follows [13]:

$$\mathbf{K}_{ij}^{\ e}=\frac{E(1-\nu)}{36V_e(1+\nu)(1-2\nu)}\begin{bmatrix} K_{xxij} & K_{xyij} & K_{xzij} \\ K_{yxij} & K_{yyij} & K_{yzij} \\ K_{zxij} & K_{zyij} & K_{zzij} \end{bmatrix} \quad (21)$$

where

$$K_{xxij}=b_ib_j+c_ic_j\frac{1-2\nu}{2(1-\nu)}+d_id_j\frac{1-2\nu}{2(1-\nu)} \quad (22\text{-a})$$

$$K_{yyij}=c_ic_j+b_ib_j\frac{1-2\nu}{2(1-\nu)}+d_id_j\frac{1-2\nu}{2(1-\nu)} \quad (22\text{-b})$$

$$K_{zzij}=d_id_j+c_ic_j\frac{1-2\nu}{2(1-\nu)}+b_ib_j\frac{1-2\nu}{2(1-\nu)} \quad (22\text{-c})$$

$$K_{xyij}=b_ic_j\frac{\nu}{(1-\nu)}+c_ib_j\frac{1-2\nu}{2(1-\nu)} \quad (22\text{-d})$$

$$K_{xzij}=b_id_j\frac{\nu}{(1-\nu)}+d_ib_j\frac{1-2\nu}{2(1-\nu)} \quad (22\text{-e})$$

$$K_{yxij}=c_ib_j\frac{\nu}{(1-\nu)}+b_ic_j\frac{1-2\nu}{2(1-\nu)} \quad (22\text{-f})$$

$$K_{yzij}=c_id_j\frac{\nu}{(1-\nu)}+d_ic_j\frac{1-2\nu}{2(1-\nu)} \quad (22\text{-g})$$

$$K_{zxij}=d_ib_j\frac{\nu}{(1-\nu)}+b_id_j\frac{1-2\nu}{2(1-\nu)} \quad (22\text{-h})$$

$$K_{zyij}=d_ic_j\frac{\nu}{(1-\nu)}+c_id_j\frac{1-2\nu}{2(1-\nu)}. \quad (22\text{-i})$$

Equation (20) is very similar to that of 3D static anisotropic magnetic analysis by using the nodal element. The consistent and interrelated property of the deformations in an elastic body can be regarded as a design increment field. In this paper, the property is used for the mesh relocation during the optimal shape design of the electromagnetic device by writing (20) as

$$[\mathbf{K}]\{\Delta x\}=\{\mathbf{f}\} \quad (23)$$

where $[\mathbf{K}]$ is the global stiffness matrix for stress analysis; $\{\Delta x\}$ is the nodal displacement, that is, the amount of relocation of the nodal coordinates $\{\mathbf{x}\}$; and $\{\mathbf{f}\}$ is a fictious load force to control the mesh density appropriately. The perturbation of the boundary can be considered as simply a displacement at the boundary. With no additional external forces and given displacements at the boundary, (23) can be used to find the displacements of the whole nodes. Equation (23) can be rewritten as follows in segmented form:

$$\begin{bmatrix} K_{bb} & K_{bd} \\ K_{db} & K_{dd} \end{bmatrix}\begin{Bmatrix} \Delta x_b \\ \Delta x_d \end{Bmatrix}=\begin{bmatrix} f_b \\ 0 \end{bmatrix} \quad (24)$$

where $\{\Delta x_b\}$ is the known perturbation of nodes on the boundary, $\{\Delta x_d\}$ is the unknown nodal displacement vector for the interior nodes, and $\{f_b\}$ is the fictitious boundary force acting on the boundary. The unknown interior nodal displacement vector can be obtained from

$$[K_{dd}]\{\Delta x_d\}=-[K_{db}]\{\Delta x_b\} \quad (25)$$

To evaluate $\{\Delta x_d\}$, we must suppress all the degrees of freedom that represent the fixed shape contour of a domain in the finite element analysis. Since this structural analysis is used merely to get a proper relocation of the interior nodes from the displacement of the surface nodes, no emphasis is placed on simulating actual deformation of a physical structure. Therefore the material parameters related to (23) could be chosen freely. To limit the computation efforts for mesh regeneration, only part of the electromagnetic analysis region can be defined as the structural analysis.

If the nodal displacements are small, the above mentioned method is sufficient to obtain a good mesh quality with smooth shape. However, when the nodal

displacements are quite large, some elements might be distorted. In this cases, a mesh smooth scheme to adapt interior nodes is suggested [14]:

$$(\mathbf{x}_n)_{new} = (1-\alpha)(\mathbf{x}_n)_{old} + \alpha \sum_{i=1}^{n_{\max}} \mathbf{x}_{ni} \Big/ n_{\max} \tag{26}$$

where node n is relocated with a specified parameter α such that $0 < \alpha \le 1$, $n_{\max}$ is the number of nodes connected to node n, and $\mathbf{x}_{ni}$ are the coordinates of node ni.

5. Numerical Shape Optimization Examples

By integrating the finite element performance analysis, the steepest descent method with design sensitivity, and the mesh relocation method, a novel 3D shape optimal design algorithm is developed and summarized in Fig. 3 The developed algorithm is applied to the optimal design of the transformer tank shield model. The transformer tank shield models, shown in Figs. 1 and 2, are the benchmark model proposed by the Investigation Committee of the IEE of Japan for reducing the volume of the shielding plate and for constraining the maximum eddy current density J_{em} at the tank within a specified value $J_{ems}(0.24\times10^6\ A/m^2)$ to prevent the local over heating [2]. The tank plate is made of conducting steel, whose conductivity and relative permeability are $0.75\times10^7 S/m$ and 1000, respectively, while the shielding plate is made of non-conducting grain-oriented silicon steel of which the relative permeabilities are 3000 and 30 for the easy and hard axes, respectively. The exciting current has 5484 AT (12A(max), 457 turns, 60Hz).

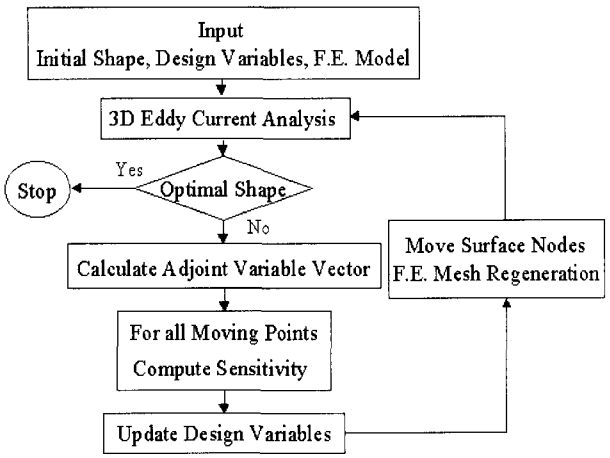

Fig. 3 The optimization system based on design sensitivity analysis

The objective function and constrains are defined as

$$F = \begin{cases} F_V = V\,[m^3] & while\ \ J_{em} < J_{ems} \\ F_J = (J_{em} - J_{em0})^2\,[A/m^2] & while\ \ J_{em} \ge J_{ems} \end{cases} \tag{27}$$

$$0 < L_1, L_2, L_3, L_4 < 0.01\ [m] \tag{28}$$

where J_{em} and J_{ems} are the computed and maximum allowable values of the maximum eddy current densities in the tank plate, respectively, and J_{em0} is set to be less than J_{ems}.

The tank shield shape is parameterized in two ways, as shown in Figs. 1 and 2, using the linear functions and step functions, respectively. In both parameterizations, the design variables are taken as the dimensions L_1, L_2, L_3, L_4, and the design sensitivities are calculated as

$$\frac{dF}{d[L]} = \beta \frac{dF_J}{d[L]} + \gamma \frac{dF_V}{d[L]} \tag{29}$$

where the coefficients (β,γ) are set to (0.7,0.3) when J_{em} is larger than J_{ems} and (0.3,0.7) when J_{em} is less than J_{ems}, respectively.

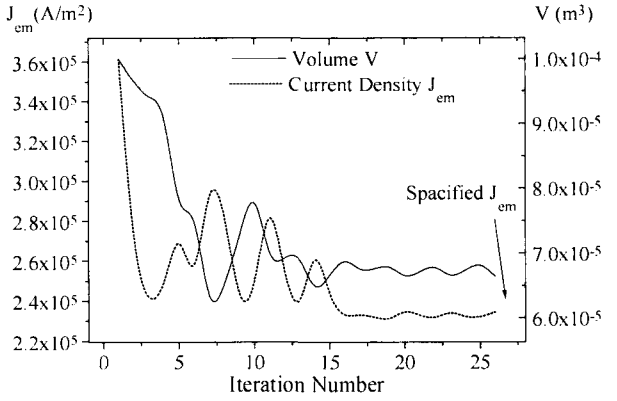

Fig. 4 The variations of the maximum eddy current density and the volume when the shape is parameterized using the linear function

When the tank shield shape is parameterized using the linear functions, the optimum result is obtained after 20 iterations. Fig. 4 shows the variations of the maximum eddy current density at the tank and the volume of the tank shield during the optimization process. It can be seen that during the first few iterations both the maximum eddy current density and the volume are reduced simultaneously, but reducing one, on the whole, makes the other increase. From the optimization experience, the coefficients in (29) may be varied for faster convergence. The initial and optimized dimensions of the tank shield are compared in

Table I, which indicates that the maximum eddy current density at the tank is kept less than the specified value while the volume of the shielding plate is much reduced. Figs. 5 and 6 compare the distributions of the magnetic flux density at the symmetric plane and the distributions of the eddy current at the tank, respectively, for the initial and optimized shapes. The relocated meshes for the shielding plate during the optimization process are shown in Fig. 7.

When the tank shield is parameterized using the step functions, the optimized shape of the shielding plate is obtained after 18 iterations. Fig. 8 shows the variations of the maximum eddy current density at the tank and the volume of the shielding plate. Note that reducing the volume while keeping the maximum eddy current density lower than the specified value is very difficult. Table II compares the dimensions of the shielding plate for the initial and optimized shapes. Since the eddy current at the tank is reduced, the eddy current loss is also reduced from 46.069[mW] with initial shape to 40.434[mW] with the optimized shape. Figs. 9 and 10 compare the distributions of the magnetic flux lines at the symmetry plane and eddy current densities on the tank, respectively, for the initial and optimized shielding plate. Fig. 11 compares the finite element meshes for the initial and final shapes of the shielding plate and shows that the original mesh topology is maintained and the relocated mesh quality is also good.

TABLE I
RESULTS OF THE SHIELD OPTIMIZATION

	L_1	L_2	L_3	L_4	V	J_{em}
		(mm)			(m^3)	(A/m^2)
Initial	2.50	2.50	2.50	2.50	1.000E-4	3.64026E5
Optimal	4.14	2.16	0.57	0.30	0.659E-4	2.35463E5

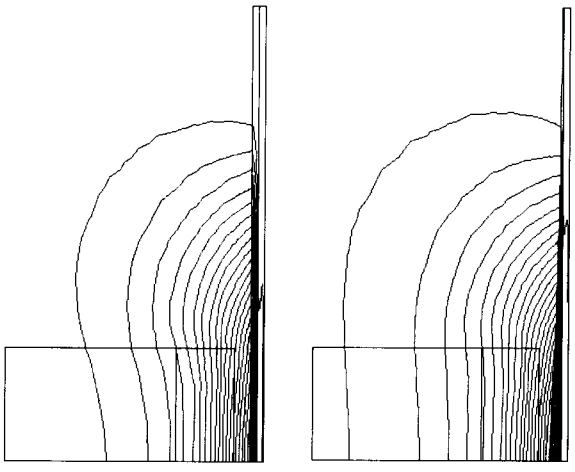

(a) (b)

Fig. 5 Distributions of the magnetic flux line. (a) with the initial shape of shielding plate, (b) with the optimized shielding plate

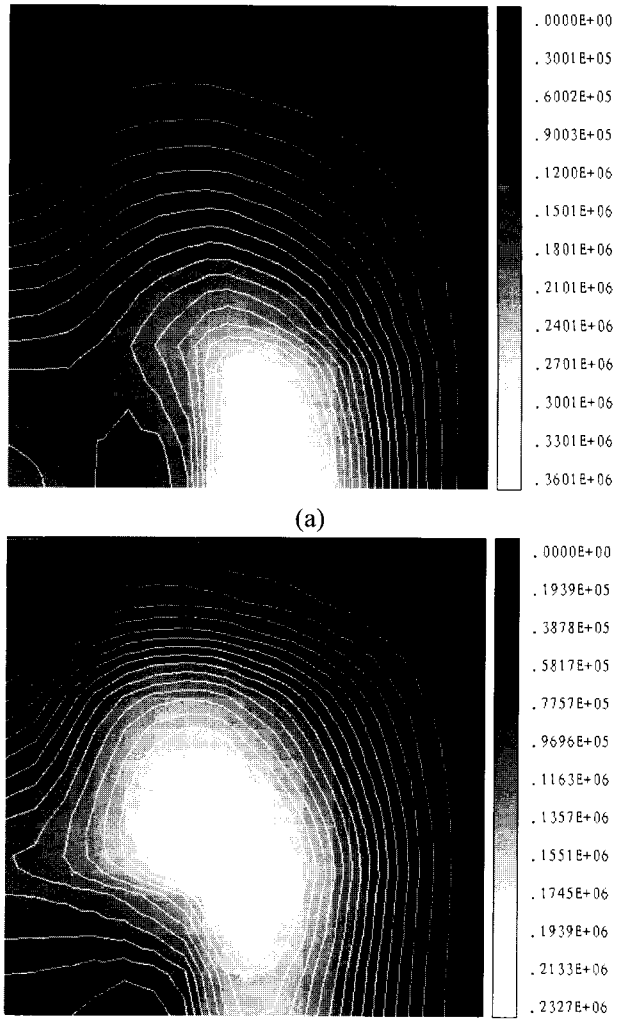

Fig. 6 Distributions of the eddy current density at the tank. (a) with the initial shape, (b) with the optimized shape

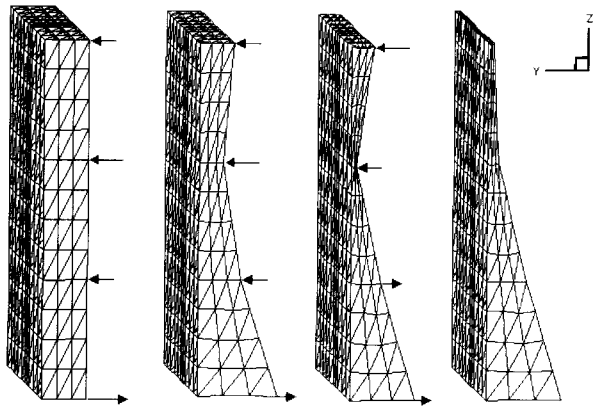

Fig. 7 The relocated meshes for the shielding plate during the optimization process, where the arrows indicate the moving directions and amounts computed from design sensitivity

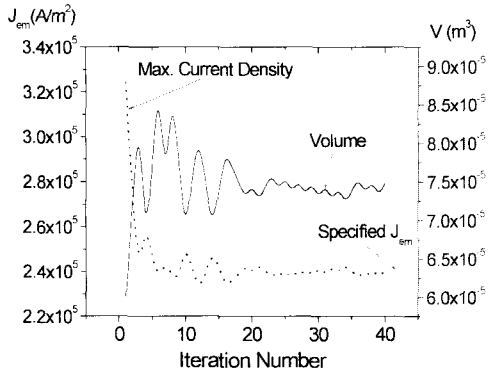

Fig. 8 The variations of the maximum eddy current density and the volume when the shielding plate is parameterized using the step functions

TABLE II

DIMENSIONS OF THE SHIELDING PLATE WHEN PARAMETERIZED USING STEP FUNCTIONS

	L_1	L_2	L_3	L_4	V	J_{em}
	(mm)				(m^3)	(A/m^2)
Initial shape	2.50	2.00	1.00	0.50	0.600E-4	3.23975E5
Optimal shape	3.44	2.29	1.27	0.49	0.749E-4	2.39120E5

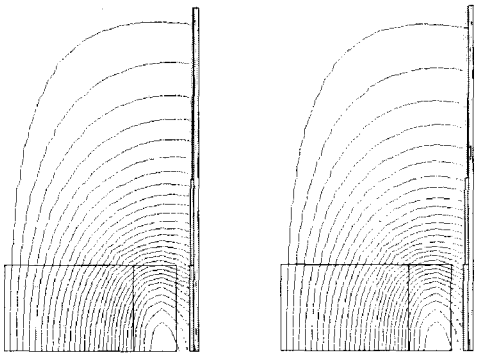

(a) (b)

Fig. 9 Distributions of the magnetic flux line; (a) with the initial shape of shielding plate, (b) with the optimized shielding plate.

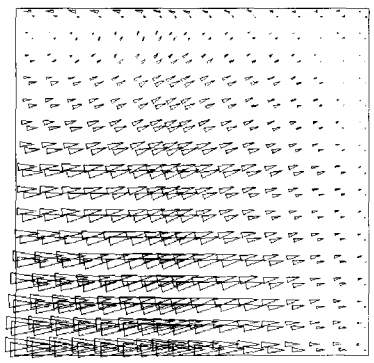

(a)

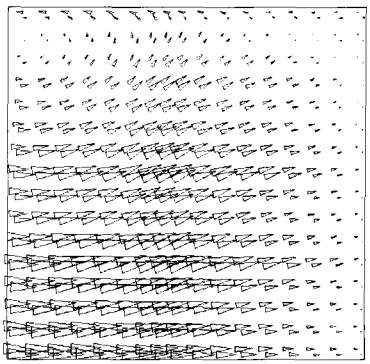

(b)

Fig. 10 Distributions of the eddy current density at the tank; (a) with the initial shape, (b) with the optimized shape.

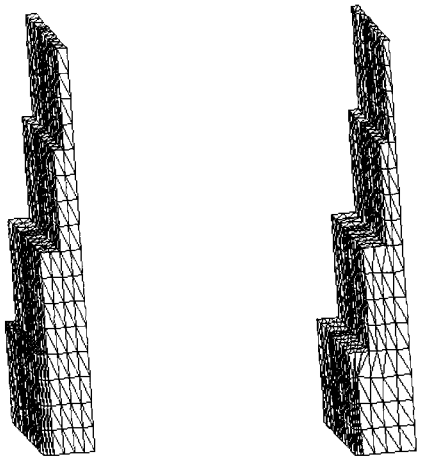

(a) (b)

Fig. 11 The relocated meshes for the shielding plate when it is parameterized using the step functions; (a) initial shape, (b) optimized shape.

6. Conclusion

A new 3D shape optimization algorithm is developed for the electromagnetic devices carrying the eddy current. In the algorithm, the 3D finite element analysis, steepest descent method with design sensitivity, and mesh relocation method are combined. The proposed method converges very fast because the method is basically a deterministic one using the gradient information from the alternating surface. Through the numerical applications to the tank shield of transformer, the strategy using the adjoint variable and design sensitivity is proven to be very effective for the 3D shape optimization with small computational efforts. The proposed mesh regeneration method is also proven successful to map the surface displacements to the finite element mesh of the body while maintaining the original mesh topology.

Acknowledgements

This work was supported in part by Korea Research Foundation under Grant No. E00150.

References

[1] S. Wang and J. Kang, "Shape optimization of BLDC motor using 3-D finite element method," *IEEE Trans. on Magn.*, Vol. 36, No. 4, pp. 1119-1123, 2000.

[2] N. Takahashi, T. Kitamura, M. Horii, J. Takehara, "Optimal design of tank shield model of transformer," *IEEE Trans. on Magn.*, Vol. 36, No. 4, pp. 1089-1093, 2000.

[3] Chang Seop Koh, Osama A. Mohammed, and Song-Yop Hahn, "Nonlinear shape design sensitivity analysis of magnetostatic problems using boundary element method," *IEEE Trans. on Magn.*, Vol. 31, No. 3, pp. 1944-1947, 1995.

[4] Jin-Kyu Byun, Kyung Choi, Hee-Succ Roh, and Song-Yop Hahn, "Optimal design procedure for a practical induction heating cooker," *IEEE Trans. on Magn.*, Vol. 36, No. 4, pp. 1390-1393, 2000.

[5] Chun-Deok Suh, Hong-Bae Lee, Song-Yop Hahn, Tae-Kyung Chung, and Il-Han Park, "Determination of levitated molten metal shape in axisymmetric induction heating system using sensitivity analysis," *IEEE Trans. on Magn.*, Vol. 31, No. 3, pp. 2158-2161, 1995.

[6] Il-Han Park, In-Gu Kwak, Hyang-Beom Lee, Ki-Sik Lee and Song-Yop Hahn, "Optimal design of transient eddy current systems driven by voltage source," *IEEE Trans. on Magn.*, Vol. 33, No. 2, pp. 1624-1629, 1997.

[7] C.S. Koh, S.Y. Hahn, K.S. Lee, and K. Choi, "Design sensitivity analysis for shape optimization of 3-D electromagnetic devices," *IEEE Trans. on Magn.*, Vol. 29, No. 2, pp. 1753-1757, 1993.

[8] S. Dappen and G. Henneberger, "A sensitivity approach for the optimization of loss efficiencies," *IEEE Trans. on Magn.*, Vol. 33, No. 2, pp. 1836-1839, 1997.

[9] Young-Seek Chung, Chang-Yul Cheon, Il-Han Park, and Song-Yop Hahn, "Optimal shape design of microwave device using FDTD and design sensitivity analysis," *IEEE Trans. on Microwave Theory and Techniques*, Vol. 48, No. 12, pp. 2289-2296, 2000.

[10] Seok-Bae Park, Hyang-Beom Lee, Song-Yop Hahn, and Il-Han Park, "Stator slot shape design of induction motors for iron loss reduction," *IEEE Trans. on Magn.*, Vol. 31, No. 3, pp. 2004-2007, 1995.

[11] Konrad Weeber and S.R.H. Hoole, "A structural mapping technique for geometric parameterization in the optimization of magnetic devices," *International Journal for Numerical Methods in Engineering*, Vol. 33, No. 10, pp. 2145-2179, 1992.

[12] O. Biro and K. Preis, "On the use of the magnetic vector potential in the finite element analysis of three-dimensional eddy currents," *IEEE Trans. On Magn.*, Vol. 25, No. 4, pp. 3145-3159, 1989.

[13] O.C. Zienkiewicz, *The Finite Element Method* (third edition), McGraw-Hill Book Company (UK), 1997.

[14] P.H. Adeli, *Advances in Design Optimization*, Chapman & Hall, 1994.

Yingying Yao

She received her B.S., M.S., and Ph.D. degrees in Electrical Engineering from the Heifei University of Technology in 1983, Chongqing University in 1987, and Shenyang University of Technology in 2000, respectively.

She is a professor at the school of electrical engineering, Shenyang University of Technology. She was a visiting scholar of the School of Electrical and Computer engineering, Chungbuk National University, Korea, from December 2001 to November 2002. Her research interests include the application of electromagnetic field analysis in power apparatus, biology medical engineering, and EMC problems. Contact her at yaoying62@ hotmail.com, (telephone) +86-24-25692028, and (fax) +86-24-25692029.

Jae Seop Ryu

He received his B.S. and M.S. degrees in Electrical Engineering from Chungbuk National University in 1997 and 1999, respectively. He is now a Ph.D. candidate of the Department of Electrical Engineering, Chungbuk National University. His research deals with the adaptive finite element method and shape optimization.

Contact him at jsryu@vod.chungbuk.ac.kr

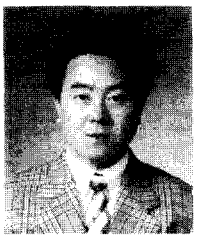

Chang Seop Koh

He received his B.S., M.S., and Ph.D. degrees in electrical engineering from Seoul National University, Seoul, Korea, in 1982, 1986, and 1992, respectively.

He was a visiting scholar of the Department of Electrical and Computer Engineering, Florida International University, USA, from May 1993 to April 1994. He was also a senior researcher at the Central Research Institute of Samsung Electro-Mechanics Co., Ltd., from May 1994 to August 1996. He has been a professor with the School of Electrical and Computer Engineering, Chungbuk National University, Korea, since 1996. His research interests include numerical analysis of electromagnetic fields using the finite element and boundary element methods, flywheel energy storage systems using high Tc superconducting material, and electric machine drives. He can be contacted at kohcs@chungbuk.ac.kr, (telephone) +82-43-261-2426, and (fax) +82-43-274-2426

Dexin Xie

She worked as a visiting scholar in the Department of Electrical and Computer Engineering, Florida International University, U.S., from 1993 to 1994. She is currently professor and Dean of School of Electrical Engineering, Shenyang University of Technology. Her research interests are computational electromagnetics and electrical engineering. She can be contacted at xiebaiy@mail.sy.ln.cn, (telephone) +86-24-25692028, and (fax) +86-24-25692029.